

Mutual Information-based Generalized Category Discovery

Florent Chiaroni *
ÉTS Montreal
Montreal, Canada

Jose Dolz
ÉTS Montreal
Montreal, Canada

Ziko Imtiaz Masud
Thales CortAIx
Montreal, Canada

Amar Mitiche
INRS
Montreal, Canada

Ismail Ben Ayed
ÉTS Montreal
Montreal, Canada

Abstract

We introduce an information-maximization approach for the Generalized Category Discovery (GCD) problem. Specifically, we explore a parametric family of loss functions evaluating the mutual information between the features and the labels, and find automatically the one that maximizes the predictive performances. Furthermore, we introduce the Elbow Maximum Centroid-Shift (EMaCS) technique, which estimates the number of classes in the unlabeled set. We report comprehensive experiments, which show that our mutual information-based approach (MIB) is both versatile and highly competitive under various GCD scenarios. The gap between the proposed approach and the existing methods is significant, more so when dealing with fine-grained classification problems. Our code: <https://github.com/fchiaroni/Mutual-Information-Based-GCD>.

1. Introduction

Deep learning methods are driving progress in a wide span of important computer vision tasks, particularly when large labeled datasets are easily accessible for training. Obtaining such large datasets is a cumbersome process, which is often a limiting factor impeding the scalability of these models. To alleviate this limitation, semi-supervised learning (SSL) has emerged as an appealing alternative, which leverages both labeled and unlabeled data to boost the performance of deep models. Despite recent success, SSL approaches work under the *closed-set* assumption, in which the categories in labeled and unlabeled subsets share the same underlying class label space. Nevertheless, this assumption rarely holds in real scenarios, where novel cat-

egories may emerge in conjunction with known classes, which typically results in significant drops in the performances of standard supervised deep learning models. Thus, the ability to detect whether the input of a deep learning model belongs or not to a set of *known* classes seen during training is essential for robust deployment in a breadth of critical application areas, such as, medicine, security, finance, agriculture, marketing, and engineering [3, 30, 33]. Thus, devising novel learning models that can address the realistic *open-set* scenario is of paramount importance.

Novel category discovery (NCD) [14, 16] tackles this problem by exploiting the knowledge learned from a set of relevant known classes to improve the clustering of the unknown categories. Nevertheless, NCD assumes the two sets of classes to be disjoint, which means that the unlabeled dataset contains only instances belonging to the set of novel categories. Generalized category discovery (GCD) [39] considers a more general scenario, where unlabeled data contain instances from both seen and novel classes. This scenario is particularly challenging, as learning is performed under class distribution mismatch, and the unlabeled data may contain categories never encountered in the available labeled set.

A main limitation of the above mentioned works is that the number of expected classes in the unlabeled set is assumed to be known during the partitioning. This may not be a realistic assumption. As a first step towards relaxing this assumption, the authors in [39] proposed to estimate the number of classes in the unlabeled set with a semi-supervised strategy, which we refer to as Max-ACC across this article. Yet, they did not use it for the partitioning experiments, and we found that Max-ACC presents some limitations.

Contributions: In this work, we consider addressing the generalized category discovery task from an information

*Corresponding author: florent.chiaroni.1@etsmtl.net

theoretic perspective. Our contributions can be summarized as follows:

- We introduce a *Mutual Information-Based* approach for GCD, which we refer to as MIB. Specifically, we explore a parameterized family of loss functions, each evaluating weighted mutual information between the features and the labels, subject to supervision constraints from the labeled samples. Each loss in the family integrates three complementary terms: *i)* a cross-entropy on the labeled points, *ii)* the entropy of posterior predictions on the unlabeled samples, and *iii)* the entropy of class marginals on the whole dataset. Our formulation is model-agnostic and could be used in conjunction with any feature extractor.
- We introduce *Elbow Maximum Centroid-Shift* (EMaCS) technique, which automatically estimates the number of classes in the unlabeled set.
- Extensive experiments demonstrate empirically the superiority of our method MIB, which consistently sets new state-of-the-art performance across six different datasets, with larger gaps on the more challenging fine-grained benchmarks. In addition, our complementary technique EMaCS also outperforms state-of-the-art GCD in finding the correct number of novel categories in unlabeled data. Furthermore, we demonstrate that the complete proposed framework achieves high performance even when the number of classes is unknown.

2. Related work

Semi-supervised learning (SSL) has been widely explored in the machine learning and computer vision community. This learning paradigm aims at leveraging large unlabeled datasets that contain the same set of classes as the labeled samples. Due to their satisfactory performance, consistency-based approaches have gained popularity recently, such as Mean-Teacher [36], MixMatch [4], UDA [42] or FixMatch [34]. An interesting alternative is self-training, which relies on the generation of pseudo-labels from a small amount of labeled data [32, 46], or in solving surrogate classification tasks [12, 43]. Nevertheless, the main limitation is that most existing SSL models rely on the closed-set assumption, failing to learn on unlabeled data points sampled from novel semantic categories.

Novel Class Discovery (NCD), which was formalized in [16], relaxes the closed-set assumption, as it focuses on discovering new categories in the unlabeled set by leveraging the knowledge learned from the labeled set. AutoNovel [15] (also referred to as RankStats) resorts to ranking statistics as an efficient approach for NCD. First, a good embedding is learned in a self-supervised manner for learning the

early feature representation layers, which is followed by a supervised fine-tuning step with labeled samples for learning high level feature representations. Finally, to determine whether two instances from the unlabeled set are from the same category, a robust ranking statistics approach is introduced. A dual ranking statistics method coupled with mutual knowledge distillation is further proposed in [45]. OpenMix [48] showed that mixing up both labeled and unlabeled data can prevent the representation learning model from overfitting the labeled categories. Some other methods [20, 47] adopt contrastive learning for the novel category discovery task. UNO [11] unifies a cross-entropy loss to jointly train the model with both the labeled and unlabeled data. Despite the good performance on discovering new categories, these methods assume that the test dataset only contains instances from the novel classes. A recent work by [44] presented a method based on a mutual-information measure, which is different from the discriminative and constrained mutual information we introduce in this work. The mutual information in [44] evaluates the relation between the old and novel categories in the label space, arguing that maximizing such a measure promotes transferring semantic knowledge. In our case, we maximize the mutual information between the feature and label spaces, on both labeled and unlabeled samples.

Generalized Category Discovery (GCD) extends NCD by allowing both old and new classes to coexist in the unlabeled dataset. This pragmatic yet challenging scenario was first presented in [39]. In this work, they propose to fine-tune a pre-trained DINO ViT [8] with one supervised and one self-supervised contrastive term. Then, a semi-supervised clustering is proposed for the label assignment. Note that, while UNO [11] and RankStats [15] are originally proposed for the NCD task, they are adapted for GCD in [39], resulting in UNO+ and RankStats+, respectively. We found that a recent work [7] addresses a similar problem, naming it *open world semi-supervised learning*. This approach consists of controlling the intra-class variance of the seen classes to align and reduce the learning gap w.r.t. novel categories.

Maximizing mutual information. Our discriminative partitioning approach MIB is built on the general and well-known *info-max* principle [28], which prescribes maximizing the mutual information (MI) between the inputs and outputs of a system. Several variants of this principle have been recently used in learning and vision tasks, including deep clustering [18, 19, 24], few-shot learning [6], representation learning [2, 17, 21, 37], deep metric learning [5] and domain adaptation [31]. Nevertheless, to the best of our knowledge, addressing the GCD problem from an information-theoretic perspective remains unexplored.

3. Proposed framework

3.1. Generalized Category Discovery problem

Assume we are given a dataset \mathcal{D} composed of two subsets so that $\mathcal{D} = \mathcal{D}_L \cup \mathcal{D}_U$. First, $\mathcal{D}_L = \{(\mathbf{x}_i, \mathbf{y}_i)\}_{i=1}^N$ refers to a labeled subset containing N images from a set of known classes in \mathcal{Y}_L . For each image \mathbf{x}_i in \mathcal{D}_L , we have access to its corresponding one-hot vector label $\mathbf{y}_i = (y_{i,k})_{1 \leq k \leq K^{\text{old}}}$, where $K^{\text{old}} = |\mathcal{Y}_L|$ is the number of classes in \mathcal{Y}_L . $y_{i,k} = 1$ if \mathbf{x}_i belongs to class k , and 0 otherwise. Now, let $\mathcal{D}_U = \{\mathbf{x}_i\}_{i=1}^M$ denote the unlabeled subset, which contains M images from a set of classes \mathcal{Y}_U composed of known classes, as well as novel classes, i.e., $\mathcal{Y}_L \subset \mathcal{Y}_U$. Note that, during inference, $K = |\mathcal{Y}_U|$ is the total number of classes, which contains both known and novel categories.

Given this setting, the Generalized Category Discovery (GCD) task introduced in [39] consists in partitioning¹ the images in the unlabeled set into separate clusters at test time. Each obtained cluster is supposed to represent a separate known or novel category. In other words, the GCD problem amounts to jointly solve (i) a semi-supervised classification task for the known classes; and (ii) a clustering task for the novel classes.

3.2. Maximizing Mutual Information (MI)

Let us denote $g_\theta : \mathcal{D} \rightarrow \mathcal{Z} \subset \mathbb{R}^D$ as the trained encoder responsible for mapping an input image \mathbf{x}_i into a feature vector \mathbf{z}_i of dimension D , with θ the set of trainable parameters and \mathcal{Z} the set of embedded features. We now define a soft partitioning model $f_{\mathbf{W}} : \mathcal{Z} \rightarrow [0, 1]^K$, which is parameterized by the weight matrix $\mathbf{W} = (\mathbf{w}_k)_{1 \leq k \leq K}$, where $\mathbf{w}_k = (w_{k,n})_{1 \leq n \leq D}$ denote its trainable parameters. For each input feature map \mathbf{z}_i , $f_{\mathbf{W}}$ outputs a softmax prediction vector $\mathbf{p}_i = (p_{i,k})_{1 \leq k \leq K}$ of dimension K , defined on the standard $(K - 1)$ -probability simplex domain $\Delta^{K-1} = \{\mathbf{p}_i \in [0, 1]^K \mid \mathbf{p}_i^T \mathbf{1} = 1\}$. Note that, similarly to the prior work in [39], we assume the number of clusters during the partitioning task to be known.

Let $Z \in \mathbb{R}^D$ denote a random variable representing the feature map. Z follows $\mathbb{P}(Z)$, which denotes the distribution of the set of embedded features \mathcal{Z} . Hence, each feature map data point \mathbf{z}_i is a realization of Z . Let $Y \in \mathcal{Y} = \{1, \dots, K\}$ be the random variable following the dataset label distribution $\mathbb{P}(Y)$.

Conditional distribution. We define $\mathbb{P}(Y|Z; \mathbf{W})$ as the conditional probability distribution modeling the outputs of our partitioning model $f_{\mathbf{W}}$, given its parameters \mathbf{W} and the input random variable Z . Thus, we can consider the softmax prediction \mathbf{p}_i as a probability simplex point where

¹We use the term *partitioning* to refer jointly to the classification task for the known classes and the clustering task for the novel classes.

each $p_{i,k} = \mathbb{P}(Y = k|Z = \mathbf{z}_i; \mathbf{W})$ denotes the conditional probability realization that data point \mathbf{z}_i belongs to class k .

Marginal distributions. Let $\boldsymbol{\pi} = (\pi_k)_{1 \leq k \leq K}$, where $\pi_k = \mathbb{P}(Y = k; \mathbf{W})$, denote the marginal distributions that we can approximate by the soft² proportion of points within each cluster, via Monte-Carlo estimation, as follows:

$$\begin{aligned} \pi_k &= \int_{\mathcal{Z}} \mathbb{P}(Z = \mathbf{z}) \mathbb{P}(Y = k|Z = \mathbf{z}; \mathbf{W}) d\mathbf{z} \\ &\approx \frac{1}{|\mathcal{Z}|} \sum_{i \in \mathcal{Z}} \mathbb{P}(Y = k|Z = \mathbf{z}_i; \mathbf{W}) = \frac{1}{|\mathcal{Z}|} \sum_{i \in \mathcal{Z}} p_{i,k}. \end{aligned} \quad (1)$$

Mutual Information. The mutual information between the labels and the features maps can be written as follows:

$$I(Y, Z) = \mathcal{H}(Y) - \mathcal{H}(Y|Z), \quad (2)$$

with $\mathcal{H}(Y)$ referring to the entropy of the marginal distributions $\mathbb{P}(Y = k; \mathbf{W})$, and $\mathcal{H}(Y|Z)$ referring to the entropy of the conditional probability distribution $\mathbb{P}(Y|Z; \mathbf{W})$.

Marginal entropy. The marginal entropy term $\mathcal{H}(Y)$ in (2) can be estimated, w.r.t. the soft marginal distributions approximation in (1), as follows:

$$\begin{aligned} \mathcal{H}(Y) &= - \sum_{k=1}^K \mathbb{P}(Y = k; \mathbf{W}) \log \mathbb{P}(Y = k; \mathbf{W}) \\ &= - \sum_{k=1}^K \pi_k \log \pi_k. \end{aligned} \quad (3)$$

Note that we can write this term, up to a constant, as the Kullback-Leibler (KL) divergence between the marginal probabilities of predictions and the uniform distribution. Thus, this marginal entropy can be used as a measure of class balance.

Conditional entropy. The conditional entropy $\mathcal{H}(Y|Z)$ can be approximated with Monte-Carlo estimation as follows:

$$\begin{aligned} \mathcal{H}(Y|Z) &\equiv \int_{\mathcal{Z}} \mathbb{P}(Z = \mathbf{z}) \mathcal{H}(\mathbb{P}(Y|Z = \mathbf{z}; \mathbf{W})) d\mathbf{z} \\ &\approx - \frac{1}{|\mathcal{Z}|} \sum_{i \in \mathcal{Z}} \sum_{k=1}^K p_{i,k} \log p_{i,k}. \end{aligned} \quad (4)$$

In essence, conditional entropy measures the uncertainty of the model's predictions. Therefore, minimizing this term

²We use the term *soft* because we estimate the proportions directly on the softmax predictions, instead of using hard labels.

encourages confident predictions. However, it is worth noting that an optimal solution for the conditional entropy minimization could assign every example to the same class with maximum certainty, i.e. assigning all data points to the same vertex of the simplex. This may yield degenerate one-class solutions in the context of our GCD multi-class task, where there could be several distinct classes in the target dataset. From this perspective, the mutual information in (2) could be interpreted as a joint measure of the prediction confidence of our model (driven by the conditional entropy), and of class balance (governed by the marginal entropy).

Based on the above identified attributes of the mutual information, we propose to maximize a family of weighted versions of $I(Y, Z)$ w.r.t \mathbf{W} for a given dataset \mathcal{Z} , while imposing supervision constraints from the set of labeled samples. Indeed, minimizing the conditional entropy term maximizes the certainty of our model predictions, whereas maximizing the marginal entropy encourages class balance, preventing degenerate solutions.

3.3. Proposed formulation

3.3.1 Constrained MI maximization

In the presented GCD scenario, we have access to a labeled subset \mathcal{D}_L , from which the subset of features \mathcal{Z}_L is derived. Thus, we propose to maximize a constrained version of the mutual information presented in (2), integrating supervision constraints on the conditional probabilities \mathbf{p}_i of the samples within the labeled set. Our constrained information maximization reads:

$$\begin{aligned} \max_{\mathbf{W}} \mathcal{H}(Y) - \underbrace{\mathcal{H}(Y|Z)}_{\text{CE}} \\ \text{s.t. } \mathbf{y}_i = \mathbf{p}_i \quad \forall \mathbf{z}_i \in \mathcal{Z}_L \end{aligned} \quad (5)$$

It is straightforward to notice that by plugging the equality constraints in (5) into the mutual information, one could write the objective as follows:

$$\min_{\mathbf{W}} \sum_{k=1}^K \pi_k \log \pi_k - \frac{1}{|\mathcal{Z}|} \sum_{i \in \mathcal{Z}} \sum_{k=1}^K h_{i,k} \log p_{i,k}, \quad (6)$$

where $h_{i,k} = y_{i,k}$ if $\mathbf{z}_i \in \mathcal{Z}_L$ and $h_{i,k} = p_{i,k}$ otherwise. That is, for $\mathbf{y}_i = \mathbf{p}_i \quad \forall \mathbf{z}_i \in \mathcal{Z}_L$, the objectives in (5) and (6) are equal to each other. Interestingly, the terms corresponding to $h_{i,k} = y_{i,k}$ in (6) yield the standard cross-entropy (CE) loss for the labeled samples. This CE loss could be viewed as *penalty* function for imposing constraints $\mathbf{y}_i = \mathbf{p}_i \quad \forall \mathbf{z}_i \in \mathcal{Z}_L$, as it reaches its minimum when these constraints are satisfied. Therefore, we do not need to impose explicitly the equality constraints in (5). Notice that, for the labeled samples, CE in (6) replaced the conditional entropy term in the mutual information. This is reasonable as CE enables to jointly impose the supervision

constraints, while encouraging implicitly confident predictions, as it pushes them toward one vertex of the simplex. Both CE and conditional entropy reach their minima at the vertices of the simplex.

3.3.2 Exploring a family of weighted MI losses

Thus, in practice, we propose to explore a family of weighted versions of the MI objective in (6), which we parameterize with a weighting factor λ :

$$\begin{aligned} \min_{\mathbf{W}} \underbrace{\sum_{k=1}^K \pi_k \log \pi_k}_{\mathcal{H}(Y)} - \underbrace{\frac{1}{|\mathcal{Z}_L|} \sum_{i \in \mathcal{Z}_L} \sum_{k=1}^K y_{i,k} \log p_{i,k}}_{\text{CE}} \\ - \underbrace{\frac{\lambda}{|\mathcal{Z}_U|} \sum_{i \in \mathcal{Z}_U} \sum_{k=1}^K p_{i,k} \log p_{i,k}}_{\mathcal{H}(Y|Z)}. \end{aligned} \quad (7)$$

Hyper-parameter $\lambda \in (0, 1]$ balances the contribution of the last unsupervised loss term in our formulation. Thus, the conditional entropy term in our MI formulation is decomposed into two terms: *i*) a cross-entropy on the set of labeled points, and *ii*) an unsupervised conditional entropy $\mathcal{H}(Y|Z)$ on the set of unlabeled points.

Note that we separately normalize the last two terms in (7) because of the following practical reason. This prevents from altering the effect of the supervision constraints (i.e. the CE term) depending on the proportion of the unlabeled samples. In situations where the number of unlabeled points is much higher than the number of labeled ones, this could drastically inhibit the supervision knowledge in our objective, reducing it into an unsupervised loss.

3.3.3 Automatic finding of the best MI loss

The loss function presented in (7) introduces the hyper-parameter λ , which controls the effect of the unsupervised $\mathcal{H}(Y|Z)$ (last term). However, introducing such a hyper-parameter could bias (either positively or negatively) our model effectiveness depending on the dataset distribution. Thus, we propose to automatically estimate the optimal weighting value as follows. We select the optimal λ value which maximizes the clustering performance on the labeled subset \mathcal{Z}_L , as we found empirically that this value simultaneously maximizes the partitioning performances on the unlabeled subset \mathcal{Z}_U . During the search for λ , we remove the cross-entropy term in (7) in order to amplify the performance variation on the labeled set across different λ values.

3.4. Finding the number of classes

Complementary to the partitioning task, we now propose a novel strategy to estimate the number of classes, which addresses some of the limitations identified in Max-ACC [39].

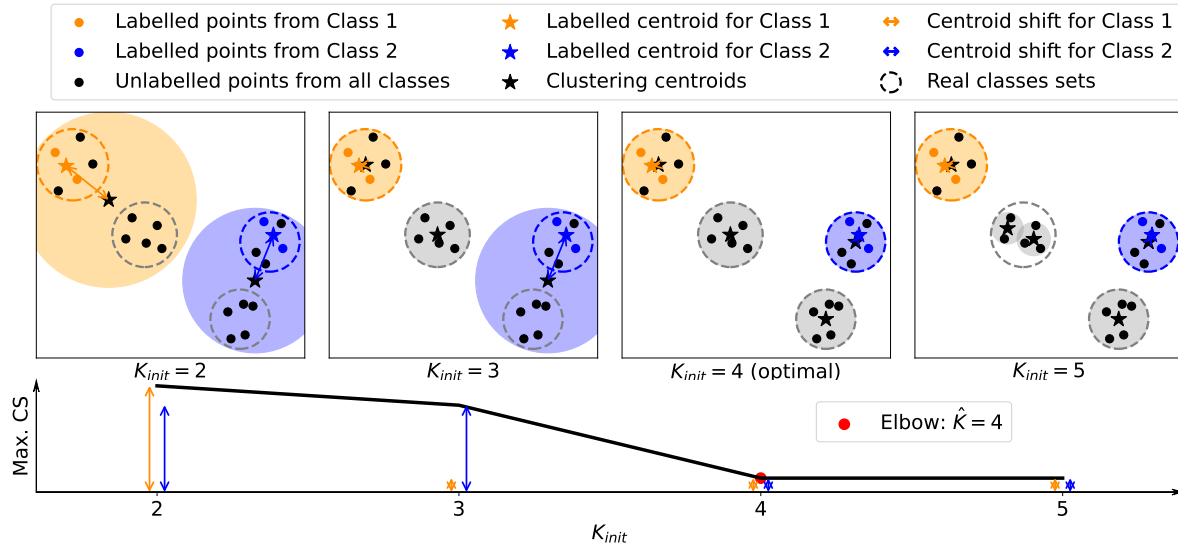


Figure 1. **Proposed Elbow Maximum Centroid-Shift (EMaCS) strategy.** The first row represents the unsupervised clustering solutions depending on the initialized number of clusters K_{init} on a given hypothetical two-dimensional feature map dataset composed of two known and two novel classes. The second row represents the curve of the related Maximum Centroid-Shift (denoted as Max. CS) for each corresponding K_{init} value. The obtained Elbow point in red has the horizontal coordinate \hat{K} , which actually corresponds to the real number of classes. In contrast, one can note that the clustering accuracy on the labeled points in this situation would be equal to one throughout all K_{init} , such that Max-ACC strategy [39] would be ineffective.

For example, if the labeled points are correctly partitioned into separate clusters, which also contain examples from novel classes, then the accuracy on the labeled points would be maximum (i.e. equal to one), despite the fact that these clusters would contain more than one class. Figure 1 illustrates such a potential drawback. Motivated by this issue, we propose a robust alternative to Max-ACC [39], which we refer to as *Elbow Maximum Centroid-Shift* (EMaCS). The three main steps of EMaCS are detailed below:

(1) **Unsupervised clustering for each possible K :** We first perform clustering on the full dataset \mathcal{Z} for each potential K in an unsupervised manner using our mutual information based partitioning model MIB. Specifically, we use *k-means* to initialize our model prototypes, and we remove the CE term on the labeled points during training. In the first row in Fig. 1, we illustrate different clustering solutions depending on several K initialization values (K_{init}) on a hypothetical two-dimensional feature map dataset containing examples from two known and two novel classes.

(2) **Maximum centroid-shift (CS) estimation for each possible K :** Then, we assign each labeled prototype (i.e., mean centroids estimated using only the labeled points for each known class) with the closest clustering prototype using the Hungarian algorithm [27], which is an optimal transport strategy. After this, we estimate the centroid-shift between each labeled prototype and the closest clustering prototype (computed in the previous step) using Euclidean distance. Then, we keep only the maximum centroid shift for

each K_{init} and draw the resulting curve, where the horizontal axis represents each K_{init} , and the vertical axis represents the maximum centroid-shift. The second row in Fig. 1 illustrates this curve.

(3) **Elbow estimation:** Finally, one can observe that the curve in Fig. 1 sharply stops decreasing when every cluster assigned with a known class only contains examples from this class. We hypothesize that the clusters found for the novel classes are simultaneously more consistent at this point. Indeed, we would like to point to the optimal clustering solution with $K_{init} = 4$ on the first row and its corresponding point in the curve denoted in red, which we refer to as the Elbow point. Specifically, Elbow is the point corresponding to the horizontal coordinate for our postulated optimal number of classes \hat{K} . In fact, the Elbow point could be found by estimating the maximum of the second derivative of the curve. However, the curve may be very noisy in practice when dealing with complex natural images, eventually along challenging fine-grained datasets³. Instead, we found more robust to select the farthest point below the line passing through the first point and the last point of the curve w.r.t Euclidean distance. Note that, the latter technique also enables the application of Brent’s algorithm during the Elbow point search, hence reducing the computational cost.

³Figure 4 in Appendix A.3 provides the curves and Elbow points which we empirically obtain for each dataset.

4. Experiments

4.1. Experiments setting

Datasets. We evaluate and compare our approach to GCD state-of-the-art approaches across six different natural image datasets. More concretely, this includes three well-known generic object recognition datasets CIFAR10 [26], CIFAR100 [26], ImageNet-100 [9], as well as the recent semantic shift benchmark suite (SSB) [38] which is composed of the three fine-grained datasets CUB [41], Stanford Cars [25] and Herbarium19 [35]. Note that the datasets on SSB bring an additional challenge to the performance of the baselines. CUB and Stanford Cars contain fine-grained categories, which are arguably harder to distinguish than generic object classes. Herbarium19 is a long-tailed dataset, which reflects a real-world use-case with large class imbalance, large intra-class and low inter-class variations.

We follow the original GCD setting [39] to split the original training set of each dataset into labeled and unlabeled subsets. More concretely, half of the image samples corresponding to the K^{old} known classes are assigned to the labeled subset, whereas the remaining half are assigned to the unlabeled subset. The latter also contains all the image samples from the remaining classes present in the original dataset, which we consider as the novel classes. In this way, the unlabeled subset is composed of instances from K different classes⁴.

Evaluation protocol. To evaluate our model we follow the evaluation protocol presented in GCD [39]. In particular, for the partitioning task, we first employ the Hungarian algorithm to solve the optimal cluster-to-class assignment jointly on both known and novel class examples, i.e. for all the predicted clusters at once. Note that our partial semi-supervised training already enables to correctly align beforehand the clusters corresponding to the known classes with real-class labels. Then, we use this optimal label-assignment solution to estimate the overall partitioning accuracy (ACC) for all classes (ALL), for known classes (OLD), and for novel classes (NEW). In the evaluation, we also report the estimated number of classes \hat{K} in the unlabeled set and the corresponding error $Err = \frac{|\hat{K}-K|}{K}$, with K the real number of classes for each dataset.

Implementation details:

- **Encoder g_θ :** As in [39], we employ the vision transformer ViT-B-16 [10] as our backbone encoder g_θ (i.e. the feature extractor). It is first pre-trained on the unlabeled dataset ImageNet [9] with DINO [8]

⁴Table 5 in Appendix A.1 provides further details on the selected number of classes, as well as the number of examples respectively present in each subset.

self-supervision. Then, it is fine-tuned on each GCD dataset of interest with a semi-supervised contrastive loss composed of an unsupervised noise contrastive term [13] and a supervised contrastive term [22]. It is empirically demonstrated in [39] that this pre-training procedure achieves robust feature representations. The resulting feature dimension is 768 per input image.

- **Partitioning model f_W :** Our partitioning model follows the architecture of a standard linear classifier. We first initialize f_W prototypes W with the centroids produced by the semi-supervised k-means (ssKM) clustering model⁵ on the entire feature map set \mathcal{Z} . The maximum number of clustering iterations for ssKM is set to 100. Then, we train f_W with the standard Adam optimizer [23], with a learning rate of 0.001 and a weight decay of 0.01, for 1000 epochs during the partitioning task, but only for 500 epochs during the search of \hat{K} in order to reduce the computational cost. We set the training batch size equal to the size of the dataset which is quite feasible in terms of memory and computation since our approach only requires the pre-computed feature maps.
- **Conditional entropy weight λ :** During the search of the number of classes with the proposed EMaCS approach, we simply set⁶ $\lambda = 1$ for the unsupervised discriminative clustering step (1) detailed in Sec. 3.4. However, during the partitioning task where the number of classes is fixed, i.e. with K assumed to be known or to be equal to \hat{K} , we automatically select the optimal value for λ in the interval $(0, 1]$ which maximizes the clustering ACC on the labeled subset, as previously detailed in Sec. 3.3.3.

4.2. Main results

In this section, we perform a comprehensive empirical evaluation of our method and compare it to GCD [39], as well as several adapted state-of-the-art approaches in related settings. In particular, RankStats+ and UNO+ are the adapted versions from RankStats [15] and UNO [11], which were originally developed for the NCD task. Furthermore, results when applying simply *k-means* [29] on the raw extracted features from DINO are also reported.

Partitioning task. For the first series of experiments, we focus on the partitioning task. We assume the real number of classes K is already estimated, following the original GCD setting [39]. The label assignment ACC on the unlabeled samples obtained by the different approaches is reported on Tab. 1. Our approach MIB yields performance

⁵Appendix A.2 provides a description of ssKM.

⁶Table 9 in Appendix A.3 complementary includes the empirical estimates of the number of classes when fixing the lower value $\lambda = 0.1$.

APPROACH	CIFAR10			CIFAR100			IMAGENET-100			CUB			STANFORD CARS			HERBARIUM19		
	ALL	OLD	NEW	ALL	OLD	NEW	ALL	OLD	NEW	ALL	OLD	NEW	ALL	OLD	NEW	ALL	OLD	NEW
K-MEANS	83.6	85.7	82.5	52.0	52.2	50.8	72.7	75.5	71.3	34.3	38.9	32.1	12.8	10.6	13.8	12.9	12.9	12.8
RANKSTATS+ [15] (TPAMI-21)	46.8	19.2	60.5	58.2	77.6	19.3	37.1	61.6	24.8	33.3	51.6	24.2	28.3	61.8	12.1	27.9	55.8	12.8
UNO+ [11] (ICCV-21)	68.6	98.3	53.8	69.5	80.6	47.2	70.3	95.0	57.9	35.1	49.0	28.1	35.5	70.5	18.6	28.3	53.7	14.7
GCD [39] (CVPR-22)	91.5	97.9	88.2	70.8	77.6	57.0	74.1	89.8	66.3	51.3	56.6	48.7	39.0	57.6	29.9	35.4	51.0	27.0
MIB (PROPOSED)	94.7	97.4	93.3	78.3	84.2	66.5	83.1	95.3	77.0	62.7	75.7	56.2	43.1	66.9	31.6	42.3	56.1	34.8

Table 1. **Generalized Category Discovery partitioning.** Partitioning ACC scores across generic and fine-grained datasets.

	CIFAR10	CIFAR100	IMAGENET-100	MEAN
	$\hat{K}(Err)$	$\hat{K}(Err)$	$\hat{K}(Err)$	(Err)
GROUND TRUTH	10 (-)	100 (-)	100 (-)	(-)
MAX-ACC [39]	9 (10%)	100 (0%)	109 (9%)	(6%)
EMACS (PROPOSED)	10 (0%)	95 (5%)	108 (8%)	(4%)

	CUB	STANFORD CARS	HERBARIUM19	MEAN
	$\hat{K}(Err)$	$\hat{K}(Err)$	$\hat{K}(Err)$	(Err)
GROUND TRUTH	200(-)	196(-)	683(-)	(-)
MAX-ACC [39]	231 (16%)	230 (15%)	520 (24%)	(18%)
EMACS (PROPOSED)	193 (4%)	207 (6%)	564 (17%)	(9%)

Table 2. **Estimation of the number of classes** in the unlabeled set.

improvements ranging from 3% on CIFAR10, where GCD already provides a high ACC score, up to 11% on CUB. Indeed, the proposed approach achieves larger improvements on those datasets that are arguably more complex.

Furthermore, it is interesting to note that the performance improvement is typically higher on novel classes. This phenomenon could be due to the interplay between both conditional and marginal entropy in our learning objective. Indeed, the conditional entropy fosters confident predictions for the unlabeled points by pushing them far from the decision boundary, so that the clustering assumption is enforced. On the other hand, the marginal entropy term encourages the model to provide balanced cluster proportions, hence ensuring consistent solutions. Overall, we can observe that our approach MIB significantly outperforms GCD state-of-the-art methods, with a consistent improvement when considering ALL categories.

\hat{K} METHOD	CIFAR10			CIFAR100			IMAGENET-100		
	ALL	OLD	NEW	ALL	OLD	NEW	ALL	OLD	NEW
GCD [39] MAX-ACC [39]	80.5	97.9	71.8	70.9	77.2	58.2	77.9	91.1	71.3
MIB EMACS	94.7	97.4	93.3	75.6	81.6	63.6	80.3	95.3	72.8

\hat{K} METHOD	CUB			STANFORD CARS			HERBARIUM19		
	ALL	OLD	NEW	ALL	OLD	NEW	ALL	OLD	NEW
GCD [39] MAX-ACC [39]	51.1	56.4	48.4	39.1	58.6	29.7	37.2	51.7	29.4
MIB EMACS	62.4	73.4	56.9	43.5	65.0	33.2	42.5	55.8	35.4

Table 3. **Realistic GCD partitioning.** ACC scores are obtained when \hat{K} is used as the number of expected classes.

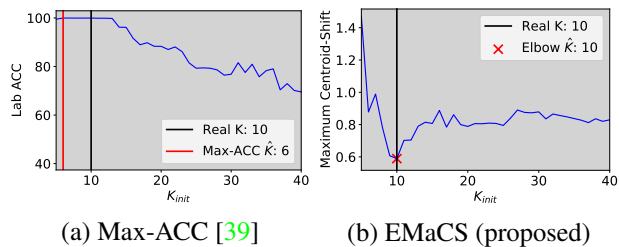


Figure 2. Graphical visualization for number of classes estimation methods on CIFAR10: (a) Max-ACC [39] and (b) The proposed EMaCS.

Estimating the number of classes. The results obtained by the proposed EMaCS strategy, compared to Max-ACC [39], are presented on Tab. 2. To obtain the results for EMaCS, we apply it by iterating throughout all potential values of K on the interval $[K^{old}, 1000]$ ⁷ also used in [39]. From these results, we can observe that the proposed EMaCS approach is overall more appropriate than Max-ACC [39] to estimate the number of classes in the unlabeled set. Furthermore, EMaCS significantly outperforms the Max-Acc strategy in the more challenging fine-grained datasets. Also, it can be observed in Fig. 2 that Max-ACC is not effective on CIFAR10 when iterating throughout all possible values of K . Specifically, Max-ACC produces the same maximum accuracy score throughout several successive K_{init} values. This coincides with the critical situation previously emphasized in Sec. 3.4, where the labeled points are correctly partitioned into separate clusters which also contain examples from novel classes. In contrast, our approach EMaCS graphically reveals an Elbow point which consistently corresponds to the real number of classes.

Performance when the number of classes is unknown. While we followed the standard practices in existing literature for the partitioning task in previous experiments, we argue that having access to the number of expected classes is an unrealistic assumption. Thus, we now relax that assumption by repeating the partitioning experiments with the estimated value of \hat{K} (See Tab. 2) instead of the real value K . These results, which are reported on Tab. 3 demonstrate

⁷Table 9 in Appendix A.3 includes complementary results when using Brent’s algorithm on the same interval.

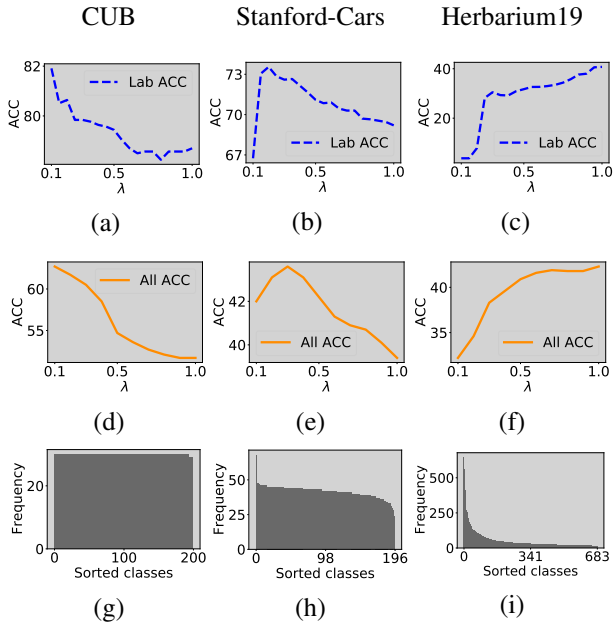


Figure 3. λ effect analysis on fine-grained datasets. The first row represents the ACC on the labeled points depending on λ value. The second row represents the ACC on all the unlabeled points depending on λ value. The third row represents the frequency of examples per class, in a sorted order.

the superiority of our method even in this more challenging scenario. This suggests that our formulation serves as a more robust solution in the absence of prior knowledge K for the GCD task.

4.3. Ablation studies

Automatic finding of optimal λ . We now motivate the interest of estimating the most appropriate λ value for each dataset by using the proposed, yet effective automatic finding strategy presented in Sec. 3.3.3. Figure 3 validates our hypothesis that selecting the λ value which maximizes the ACC on the labeled data (Lab ACC) also maximizes the ACC on all the unlabeled data (All ACC), showing the correlation between both. It is also interesting to note that a small λ value provides better results on a dataset with uniform class proportions such as CUB (see Figures 3 (a), (d), (g)), meanwhile a higher λ value is more appropriate on the long-tailed dataset Herbarium19 (see Figures 3 (c), (f), (i)). Indeed, a small weighting of the conditional entropy term in (7) accentuates the relative marginal entropy term effect. Overall, selecting λ in this way prevents from requiring the knowledge of how much long-tailed is the dataset of interest.

Effect of each loss term. We now evaluate the contribution of each term in our learning objective (7). In particular, Tab. 4 highlights the corresponding effect of the conditional entropy, the marginal entropy, and the proposed

penalty constraint (i.e. replace conditional entropy with CE on labeled points). From these results, we can draw three different observations: 1) Only minimizing the conditional entropy term produces degenerated solutions, as expected. 2) Maximizing the marginal entropy term, as well as activating the proposed constraint, prevent these undesired degenerated solutions. 3) The prediction performances are further improved when these two components are simultaneously coupled with the conditional entropy term.

LOSS TERMS USED	S.T. CONSTRAINT	CUB			STANFORD CARS			HERBARIUM19		
		ALL	OLD	NEW	ALL	OLD	NEW	ALL	OLD	NEW
$-\mathcal{H}(Y Z)$	✗	6.1	0.0	9.1	2.5	0.0	3.6	4.0	4.0	4.1
$-\mathcal{H}(Y Z)$	✓	38.6	46.2	34.8	29.8	51.3	19.5	34.6	45.4	28.9
$\mathcal{H}(Y) - \mathcal{H}(Y Z)$	✗	56.6	66.4	51.7	40.8	60.2	31.5	36.1	41.0	33.4
$\mathcal{H}(Y) - \mathcal{H}(Y Z)$	✓	62.7	75.7	56.2	43.1	66.9	31.6	42.3	56.1	34.8

Table 4. **Loss terms and constraint effects** on prediction performances (ACC) of proposed method MIB on fine-grained datasets.

5. Conclusion

In this work we propose a simple yet effective alternative for Generalized Category Discovery. In particular, we introduce a constrained mutual information maximization formulation between the learned features and their labels. The presented framework achieves new state-of-the-art results in the GCD tasks, outperforming existing solutions across the different short-tailed and long-tailed benchmarks by a significant margin. Moreover, in contrast to the prior work, we relax the assumption that the number of classes in the unlabeled set is given, which facilitates the robustness of the proposed model in this more challenging scenario. Furthermore, it is noteworthy to mention that our formulation is flexible and could, therefore, be coupled with any trained feature extractor. We hope that the proposed framework will be useful for future research and development to solve the GCD problem for real-world applications.

Limitations. A common limitation in the current GCD learning paradigm stems from the fact that the models require access to the entire target unlabeled dataset at test time. Needless to say, this strong assumption might hinder the scalability of these approaches when the target set is composed of a small number of images, or when samples appear sequentially. The existing approaches require access to the labeled set to compute the required number of clusters, which can limit their applications in scenarios with privacy concerns and restrictions on sharing data. Note that, while Max-ACC requires access to all the labeled points, our EMaCS approach would only need access to labeled centroids.

References

- [1] David Arthur and Sergei Vassilvitskii. K-means++: The advantages of careful seeding. SODA '07, page 1027–1035, USA, 2007. Society for Industrial and Applied Mathematics. [11](#)
- [2] Philip Bachman, R Devon Hjelm, and William Buchwalter. Learning representations by maximizing mutual information across views. *Advances in neural information processing systems*, 32, 2019. [2](#)
- [3] Abhijit Bendale and Terrance E Boult. Towards open set deep networks. In *Proceedings of the IEEE conference on computer vision and pattern recognition*, pages 1563–1572, 2016. [1](#)
- [4] David Berthelot, Nicholas Carlini, Ian Goodfellow, Nicolas Papernot, Avital Oliver, and Colin A Raffel. Mixmatch: A holistic approach to semi-supervised learning. *Advances in neural information processing systems*, 32, 2019. [2](#)
- [5] Malik Boudiaf, Jérôme Rony, Imtiaz Masud Ziko, Eric Granger, Marco Pedersoli, Pablo Piantanida, and Ismail Ben Ayed. A unifying mutual information view of metric learning: cross-entropy vs. pairwise losses. In *European conference on computer vision*, pages 548–564. Springer, 2020. [2](#)
- [6] Malik Boudiaf, Imtiaz Ziko, Jérôme Rony, José Dolz, Pablo Piantanida, and Ismail Ben Ayed. Information maximization for few-shot learning. *Advances in Neural Information Processing Systems*, 33:2445–2457, 2020. [2](#)
- [7] Kaidi Cao, Maria Brbic, and Jure Leskovec. Open-world semi-supervised learning. In *International Conference on Learning Representations*, 2022. [2](#)
- [8] Mathilde Caron, Hugo Touvron, Ishan Misra, Hervé Jégou, Julien Mairal, Piotr Bojanowski, and Armand Joulin. Emerging properties in self-supervised vision transformers. In *Proceedings of the IEEE/CVF International Conference on Computer Vision*, pages 9650–9660, 2021. [2](#), [6](#)
- [9] Jia Deng, Wei Dong, Richard Socher, Li-Jia Li, Kai Li, and Li Fei-Fei. Imagenet: A large-scale hierarchical image database. In *2009 IEEE conference on computer vision and pattern recognition*, pages 248–255. Ieee, 2009. [6](#)
- [10] Alexey Dosovitskiy, Lucas Beyer, Alexander Kolesnikov, Dirk Weissenborn, Xiaohua Zhai, Thomas Unterthiner, Mostafa Dehghani, Matthias Minderer, Georg Heigold, Sylvain Gelly, Jakob Uszkoreit, and Neil Houlsby. An image is worth 16x16 words: Transformers for image recognition at scale. In *International Conference on Learning Representations*, 2021. [6](#)
- [11] Enrico Fini, Enver Sangineto, Stéphane Lathuilière, Zhun Zhong, Moin Nabi, and Elisa Ricci. A unified objective for novel class discovery. In *Proceedings of the IEEE/CVF International Conference on Computer Vision*, pages 9284–9292, 2021. [2](#), [6](#), [7](#), [12](#)
- [12] Spyros Gidaris, Praveer Singh, and Nikos Komodakis. Un-supervised representation learning by predicting image rotations. In *International Conference on Learning Representations*, 2018. [2](#)
- [13] Michael Gutmann and Aapo Hyvärinen. Noise-contrastive estimation: A new estimation principle for unnormalized statistical models. In *Proceedings of the thirteenth international conference on artificial intelligence and statistics*, pages 297–304. JMLR Workshop and Conference Proceedings, 2010. [6](#)
- [14] Kai Han, Sylvestre-Alvise Rebuffi, Sebastien Ehrhardt, Andrea Vedaldi, and Andrew Zisserman. Automatically discovering and learning new visual categories with ranking statistics. *arXiv preprint arXiv:2002.05714*, 2020. [1](#)
- [15] Kai Han, Sylvestre-Alvise Rebuffi, Sebastien Ehrhardt, Andrea Vedaldi, and Andrew Zisserman. Autonovel: Automatically discovering and learning novel visual categories. *IEEE Transactions on Pattern Analysis and Machine Intelligence*, 2021. [2](#), [6](#), [7](#), [12](#)
- [16] Kai Han, Andrea Vedaldi, and Andrew Zisserman. Learning to discover novel visual categories via deep transfer clustering. In *Proceedings of the IEEE/CVF International Conference on Computer Vision*, pages 8401–8409, 2019. [1](#), [2](#)
- [17] R Devon Hjelm, Alex Fedorov, Samuel Lavoie-Marchildon, Karan Grewal, Phil Bachman, Adam Trischler, and Yoshua Bengio. Learning deep representations by mutual information estimation and maximization. *arXiv preprint arXiv:1808.06670*, 2018. [2](#)
- [18] Weihua Hu, Takeru Miyato, Seiya Tokui, Eiichi Matsumoto, and Masashi Sugiyama. Learning discrete representations via information maximizing self-augmented training. In *International conference on machine learning*, pages 1558–1567. PMLR, 2017. [2](#)
- [19] Mohammed Jabi, Marco Pedersoli, Amar Mitiche, and Ismail Ben Ayed. Deep clustering: On the link between discriminative models and k-means. *IEEE transactions on pattern analysis and machine intelligence*, 43(6):1887–1896, 2019. [2](#)
- [20] Xuhui Jia, Kai Han, Yukun Zhu, and Bradley Green. Joint representation learning and novel category discovery on single-and multi-modal data. In *Proceedings of the IEEE/CVF International Conference on Computer Vision*, pages 610–619, 2021. [2](#)
- [21] Mete Kemertas, Leila Pishdad, Konstantinos G Derpanis, and Afsaneh Fazly. Rankmi: A mutual information maximizing ranking loss. In *Proceedings of the IEEE/CVF Conference on Computer Vision and Pattern Recognition*, pages 14362–14371, 2020. [2](#)
- [22] Prannay Khosla, Piotr Teterwak, Chen Wang, Aaron Sarna, Yonglong Tian, Phillip Isola, Aaron Maschinot, Ce Liu, and Dilip Krishnan. Supervised contrastive learning. *Advances in Neural Information Processing Systems*, 33:18661–18673, 2020. [6](#)
- [23] Diederik P Kingma and Jimmy Ba. Adam: A method for stochastic optimization. *arXiv preprint arXiv:1412.6980*, 2014. [6](#)
- [24] Andreas Krause, Pietro Perona, and Ryan Gomes. Discriminative clustering by regularized information maximization. *Advances in neural information processing systems*, 23, 2010. [2](#)
- [25] Jonathan Krause, Michael Stark, Jia Deng, and Li Fei-Fei. 3d object representations for fine-grained categorization. In *Proceedings of the IEEE international conference on computer vision workshops*, pages 554–561, 2013. [6](#)

- [26] Alex Krizhevsky, Geoffrey Hinton, et al. Learning multiple layers of features from tiny images. 2009. [6](#)
- [27] Harold W Kuhn. The hungarian method for the assignment problem. *Naval research logistics quarterly*, 2(1-2):83–97, 1955. [5](#)
- [28] Ralph Linsker. Self-organization in a perceptual network. *Computer*, 21(3):105–117, 1988. [2](#)
- [29] J MacQueen. Classification and analysis of multivariate observations. In *5th Berkeley Symp. Math. Statist. Probability*, pages 281–297, 1967. [6](#), [11](#)
- [30] David Macêdo, Tsang Ing Ren, Cleber Zanchettin, Adriano L. I. Oliveira, and Teresa Ludermit. Entropic out-of-distribution detection. In *2021 International Joint Conference on Neural Networks (IJCNN)*, pages 1–8, 2021. [1](#)
- [31] Yingwei Pan, Ting Yao, Yehao Li, Chong-Wah Ngo, and Tao Mei. Exploring category-agnostic clusters for open-set domain adaptation. In *Proceedings of the IEEE/CVF Conference on Computer Vision and Pattern Recognition*, pages 13867–13875, 2020. [2](#)
- [32] Mamshad Nayeem Rizve, Kevin Duarte, Yogesh S Rawat, and Mubarak Shah. In defense of pseudo-labeling: An uncertainty-aware pseudo-label selection framework for semi-supervised learning. In *International Conference on Learning Representations*, 2020. [2](#)
- [33] Abhijit Guha Roy, Jie Ren, Shekoofeh Azizi, Aaron Loh, Vivek Natarajan, Basil Mustafa, Nick Pawlowski, Jan Freyberg, Yuan Liu, Zach Beaver, et al. Does your dermatology classifier know what it doesn’t know? detecting the long-tail of unseen conditions. *Medical Image Analysis*, 75:102274, 2022. [1](#)
- [34] Kihyuk Sohn, David Berthelot, Nicholas Carlini, Zizhao Zhang, Han Zhang, Colin A Raffel, Ekin Dogus Cubuk, Alexey Kurakin, and Chun-Liang Li. Fixmatch: Simplifying semi-supervised learning with consistency and confidence. *Advances in neural information processing systems*, 33:596–608, 2020. [2](#)
- [35] Kiat Chuan Tan, Yulong Liu, Barbara Ambrose, Melissa Tulig, and Serge Belongie. The herbarium challenge 2019 dataset. *Workshop on Fine-Grained Visual Categorization*, 2019. [6](#)
- [36] Antti Tarvainen and Harri Valpola. Mean teachers are better role models: Weight-averaged consistency targets improve semi-supervised deep learning results. *Advances in neural information processing systems*, 30, 2017. [2](#)
- [37] Michael Tschannen, Josip Djolonga, Paul K Rubenstein, Sylvain Gelly, and Mario Lucic. On mutual information maximization for representation learning. In *International Conference on Learning Representations*, 2019. [2](#)
- [38] Sagar Vaze, Kai Han, Andrea Vedaldi, and Andrew Zisserman. Open-set recognition: A good closed-set classifier is all you need. In *International Conference on Learning Representations*, 2021. [6](#)
- [39] Sagar Vaze, Kai Han, Andrea Vedaldi, and Andrew Zisserman. Generalized category discovery. In *Proceedings of the IEEE/CVF Conference on Computer Vision and Pattern Recognition*, pages 7492–7501, 2022. [1](#), [2](#), [3](#), [4](#), [5](#), [6](#), [7](#), [11](#), [12](#), [13](#)
- [40] Sagar Vaze, Kai Han, Andrea Vedaldi, and Andrew Zisserman. Generalized category discovery. *CoRR*, abs/2201.02609, 2022. [12](#)
- [41] Catherine Wah, Steve Branson, Peter Welinder, Pietro Perona, and Serge Belongie. The caltech-ucsd birds-200-2011 dataset. 2011. [6](#)
- [42] Qizhe Xie, Zihang Dai, Eduard Hovy, Thang Luong, and Quoc Le. Unsupervised data augmentation for consistency training. *Advances in Neural Information Processing Systems*, 33:6256–6268, 2020. [2](#)
- [43] Xiaohua Zhai, Avital Oliver, Alexander Kolesnikov, and Lucas Beyer. S4l: Self-supervised semi-supervised learning. In *Proceedings of the IEEE/CVF International Conference on Computer Vision*, pages 1476–1485, 2019. [2](#)
- [44] Chuyu Zhang, Chuanyang Hu, Ruijie Xu, Zhitong Gao, Qian He, and Xuming He. Mutual information-guided knowledge transfer for novel class discovery. *arXiv preprint arXiv:2206.12063*, 2022. [2](#)
- [45] Bingchen Zhao and Kai Han. Novel visual category discovery with dual ranking statistics and mutual knowledge distillation. *Advances in Neural Information Processing Systems*, 34:22982–22994, 2021. [2](#)
- [46] Mingkai Zheng, Shan You, Lang Huang, Fei Wang, Chen Qian, and Chang Xu. Simmatch: Semi-supervised learning with similarity matching. In *Proceedings of the IEEE/CVF Conference on Computer Vision and Pattern Recognition*, pages 14471–14481, 2022. [2](#)
- [47] Zhun Zhong, Enrico Fini, Subhankar Roy, Zhiming Luo, Elisa Ricci, and Nicu Sebe. Neighborhood contrastive learning for novel class discovery. In *Proceedings of the IEEE/CVF Conference on Computer Vision and Pattern Recognition*, pages 10867–10875, 2021. [2](#)
- [48] Zhun Zhong, Linchao Zhu, Zhiming Luo, Shaozi Li, Yi Yang, and Nicu Sebe. Openmix: Reviving known knowledge for discovering novel visual categories in an open world. In *Proceedings of the IEEE/CVF Conference on Computer Vision and Pattern Recognition*, pages 9462–9470, 2021. [2](#)

A. Appendix

A.1. Composition of the datasets for the GCD task

Table 5 details for each dataset the selected number of classes, as well as the number of examples respectively present in each subset, w.r.t. the generalized category discovery setting introduced in [39].

	CIFAR10	CIFAR100	IMAGENET-100	CUB	SCARS	HERBARIUM19
$ \mathcal{Y}_L $	5	80	50	100	98	341
$ \mathcal{Y}_U $	10	100	100	200	196	683
$ \mathcal{D}_L $	12.5K	20K	31.9K	1.5K	2.0K	8.9K
$ \mathcal{D}_U $	37.5K	30K	95.3K	4.5K	6.1K	25.4K

Table 5. Composition of the datasets used.

A.2. Semi-supervised k-means (ssKM)

Parameters initialization for ssKM. We denote the centroid parameters of ssKM as $\mathbf{W} = (\mathbf{W}^{old}, \mathbf{W}^{new})$, such that we have:

$$\begin{cases} \mathbf{W}^{old} = (\mathbf{w}_k^{old})_{1 \leq k \leq K^{old}} \\ \mathbf{W}^{new} = (\mathbf{w}_k^{new})_{K^{old}+1 \leq k \leq K^{old}+K^{new}} \end{cases},$$

with \mathbf{W}^{old} and \mathbf{W}^{new} the centroids for the known and novel classes, respectively. We initialize \mathbf{W} by using both the labeled set and the unlabeled set jointly. As in [39], we first produce the centroids for the known classes using the labeled set, such that: $\mathbf{w}_k^{old} = (\sum_{\mathbf{z}_i \in \mathcal{Z}_L} y_{i,k} \mathbf{z}_i) / \sum_{\mathbf{z}_i \in \mathcal{Z}_L} y_{i,k}$. Then, we initialize the centroids corresponding to the novel classes with kmeans++ initialization [1], constrained on the centroids \mathbf{W}^{old} .

ssKM objective and clustering process. As in [39], we update the cluster centroids of ssKM algorithm, with the following objective:

$$L_{ssKM}(\mathbf{Y}; \mathbf{U}; \mathbf{W}) = \left(\sum_{k=1}^K \sum_{\mathbf{z}_i \in \mathcal{Z}_L} y_{i,k} \|\mathbf{z}_i - \mathbf{w}_k\|_2 \right) + \left(\sum_{k=1}^K \sum_{\mathbf{z}_i \in \mathcal{Z}_U} u_{i,k} \|\mathbf{z}_i - \mathbf{w}_k\|_2 \right), \quad (8)$$

where $\|\cdot\|_2$ denotes the Euclidean distance, and $\mathbf{u}_i = (u_{i,k})_{1 \leq k \leq K}$ denotes the latent binary vector assigning point \mathbf{z}_i to cluster k . $\mathbf{U} \in \{0, 1\}^{NK}$ denotes the latent assignment matrix composed of the latent binary vectors. ssKM algorithm proceeds with the same block-coordinate descent approach as the standard unsupervised k-means [29]. Thus, in order to minimize L_{ssKM} , it proceeds with the following cluster assignment and centroid updates cycle:

- **U-update:** Do the label assignment of the unlabeled points such that:

$$u_{i,k} = \begin{cases} 1 & \text{if } \arg \min_k \|\mathbf{z}_i - \mathbf{w}_k\|_2 = k \\ 0 & \text{otherwise.} \end{cases}$$

- **W-update:** Find $\arg \min_{\mathbf{W}} L_{ssKM}(\mathbf{Y}; \mathbf{U}; \mathbf{W})$.

Note that the latent label assignment update step is not applied on the labeled points, for which we simply keep using the available ground-truth labels in the first term in (8), all along the clustering process.

A.3. Supplementary results

Effect of prototypes initialization. All along our article experiments, we found empirically consistent to use ssKM (detailed in Sec. A.2) centroids to initialize our MIB partitioning model prototypes. In this section, in order to endorse this choice, we empirically emphasize across Tab. 6 and Tab. 7 the effect of prototypes initialization on MIB prediction performances. We thus compare the following three different possible initializations (INIT): -SSRDM INIT consists of using labeled points for prototypes of known classes, and random points for prototypes of novel classes; -SSKM++ INIT consists of using labeled points for prototypes of known classes, and kmeans++ points for prototypes of novel classes; -SSKM INIT consists of using ssKM centroids as INIT prototypes. The results observed on Tab. 6 and Tab. 7 show that the proposed approach is overall almost insensitive to prototypes initialization. One can also note that MIB performances are slightly improved when using directly SSKM++ INIT.

	CIFAR10			CIFAR100			IMAGENET-100		
INIT	ALL	OLD	NEW	ALL	OLD	NEW	ALL	OLD	NEW
SSRDM	94.6	97.4	93.2	78.2	85.4	64.0	82.0	95.4	75.2
SSKM++	94.7	97.4	93.3	78.5	84.3	66.9	83.6	95.4	77.8
SSKM	94.7	97.4	93.3	78.3	84.2	66.5	83.1	95.3	77.0

Table 6. **Prototypes initialization effect** on MIB ACC performances on generic datasets.

	CUB			STANFORD CARS			HERBARIUM19		
INIT	ALL	OLD	NEW	ALL	OLD	NEW	ALL	OLD	NEW
SSRDM	62.1	76.2	55.1	43.0	64.3	32.7	42.7	55.3	36.0
SSKM++	64.3	76.3	58.4	43.5	65.6	32.8	42.3	55.3	35.4
SSKM	62.7	75.7	56.2	43.1	66.9	31.6	42.3	56.1	34.8

Table 7. **Prototypes initialization effect** on MIB ACC performances on fine-grained datasets.

Effect of MIB objective components on generic datasets. We can observe on Tab. 8 that the marginal entropy term, which we introduce in (7), is particularly beneficial on generic datasets CIFAR100 and IMAGENET-100.

		CIFAR10			CIFAR100			IMAGENET-100		
LOSS TERMS USED	S.T. CONSTRAINT	ALL	OLD	NEW	ALL	OLD	NEW	ALL	OLD	NEW
$-\mathcal{H}(Y Z)$	×	94.5	97.5	93.1	2.3	1.0	5.0	39.1	82.3	17.3
$-\mathcal{H}(Y Z)$	✓	94.5	97.5	93.0	66.3	73.1	52.8	54.7	85.6	39.1
$\mathcal{H}(Y) - \mathcal{H}(Y Z)$	×	94.8	97.2	93.6	78.8	82.4	71.5	83.1	93.9	77.6
$\mathcal{H}(Y) - \mathcal{H}(Y Z)$	✓	94.7	97.4	93.3	78.3	84.2	66.5	83.1	95.3	77.0

Table 8. **MIB objective components effects** on generic datasets in terms of ACC scores.

	BRENT	CIFAR10	CIFAR100	IMAGENET-100	CUB	STFRD CARS	HERBARIUM19	MEAN
		$\hat{K}(Err)$						
GROUND TRUTH	-	10(-)	100(-)	100(-)	200(-)	196(-)	683(-)	
MAX-ACC [39]	×	6 (40%)	97 (3%)	88 (12%)	238 (19%)	133 (32%)	343 (50%)	(26%)
EMACS ($\lambda = 0.1$)	×	10 (0%)	99 (1%)	97 (3%)	221 (11%)	176 (10%)	478 (30%)	(9%)
EMACS ($\lambda = 1$)	×	10 (0%)	95 (5%)	108 (8%)	193 (4%)	207 (6%)	564 (17%)	(7%)
MAX-ACC [39]	✓	9 (10%)	100 (0%)	109 (9%)	231 (16%)	230 (15%)	520 (24%)	(12%)
EMACS ($\lambda = 0.1$)	✓	10 (0%)	105 (5%)	100 (0%)	227 (14%)	181 (8%)	503 (26%)	(9%)
EMACS ($\lambda = 1$)	✓	10 (0%)	99 (1%)	88 (12%)	209 (5%)	246 (26%)	593 (13%)	(9%)

Table 9. Comparison of Max-ACC [39] with proposed EMaCS technique (see Sec. 3.4) to estimate of the number of classes in the unlabeled set for generic and fine-grained datasets.

CLASSES	\hat{K} METHOD	CIFAR10			CIFAR100			IMAGENET-100			CUB			STANFORD CARS			HERBARIUM19		
		ALL	OLD	NEW	ALL	OLD	NEW	ALL	OLD	NEW	ALL	OLD	NEW	ALL	OLD	NEW	ALL	OLD	NEW
GCD [39]	MAX-ACC [39]	56.3	58.7	55.1	70.7	77.7	56.8	72.4	87.5	64.9	50.3	54.9	48.0	35.3	53.7	26.5	36.7	50.9	29.1
GCD [39]	MAX-ACC (BRENT) [39]	80.5	97.9	71.8	70.9	77.2	58.2	77.9	91.1	71.3	51.1	56.4	48.4	39.1	58.6	29.7	37.2	51.7	29.4
MIB	EMACS ($\lambda = 0.1$)	94.7	97.4	93.3	78.0	84.7	64.5	79.9	93.3	73.2	61.7	75.1	55.0	42.4	65.4	31.3	41.5	55.2	34.2
MIB	EMACS ($\lambda = 1$)	94.7	97.4	93.3	75.6	81.6	63.6	80.3	95.3	72.8	62.4	73.4	56.9	43.5	65.0	33.2	42.5	55.8	35.4

Table 10. Partitioning ACC scores across generic and fine-grained datasets when using \hat{K} . We do not use Brent’s algorithm during EMaCS process. During MIB partitioning which uses the resulting estimated value \hat{K} , we still automatically estimate λ .

ACC- vI	APPROACH	CIFAR10			CIFAR100			IMAGENET-100			CUB			STANFORD CARS			HERBARIUM19		
		ALL	OLD	NEW	ALL	OLD	NEW	ALL	OLD	NEW	ALL	OLD	NEW	ALL	OLD	NEW	ALL	OLD	NEW
	K-MEANS	83.6	85.7	82.5	52.0	53.7	51.1	73.4	75.5	71.3	35.7	42.3	32.4	14.2	14.2	14.2	14.1	14.7	13.3
	RANKSTATS+ [15] (TPAMI-21)	84.5	96.4	78.5	65.0	78.8	37.4	50.9	94.2	29.2	37.1	73.8	18.7	29.2	53.6	17.1	31.4	54.5	18.9
	UNO+ [11] (ICCV-21)	72.4	95.0	61.1	64.1	73.8	44.8	62.3	94.7	46.0	40.1	71.1	24.5	20.6	33.7	14.1	21.2	36.1	13.3
	GCD [39] (CVPR-22)	91.5	97.9	88.2	76.9	84.5	61.7	75.1	92.2	66.5	54.0	75.4	43.4	42.0	61.2	32.4	39.4	40.5	38.5
	MIB (PROPOSED)	94.7	97.4	93.3	79.0	85.3	66.5	83.1	95.3	77.0	65.1	79.3	57.9	46.2	71.6	34.0	50.2	66.4	41.5

Table 11. Partitioning performances across generic and fine-grained datasets with the metric ACC- vI proposed in the previous version of GCD (See the first GCD pre-print [40] and public code updates <https://github.com/sgvaze/generalized-category-discovery>), where the optimal cluster-to-class label assignment is performed separately for old and novel classes. This assignment process may not be appropriate in real-scenarios.

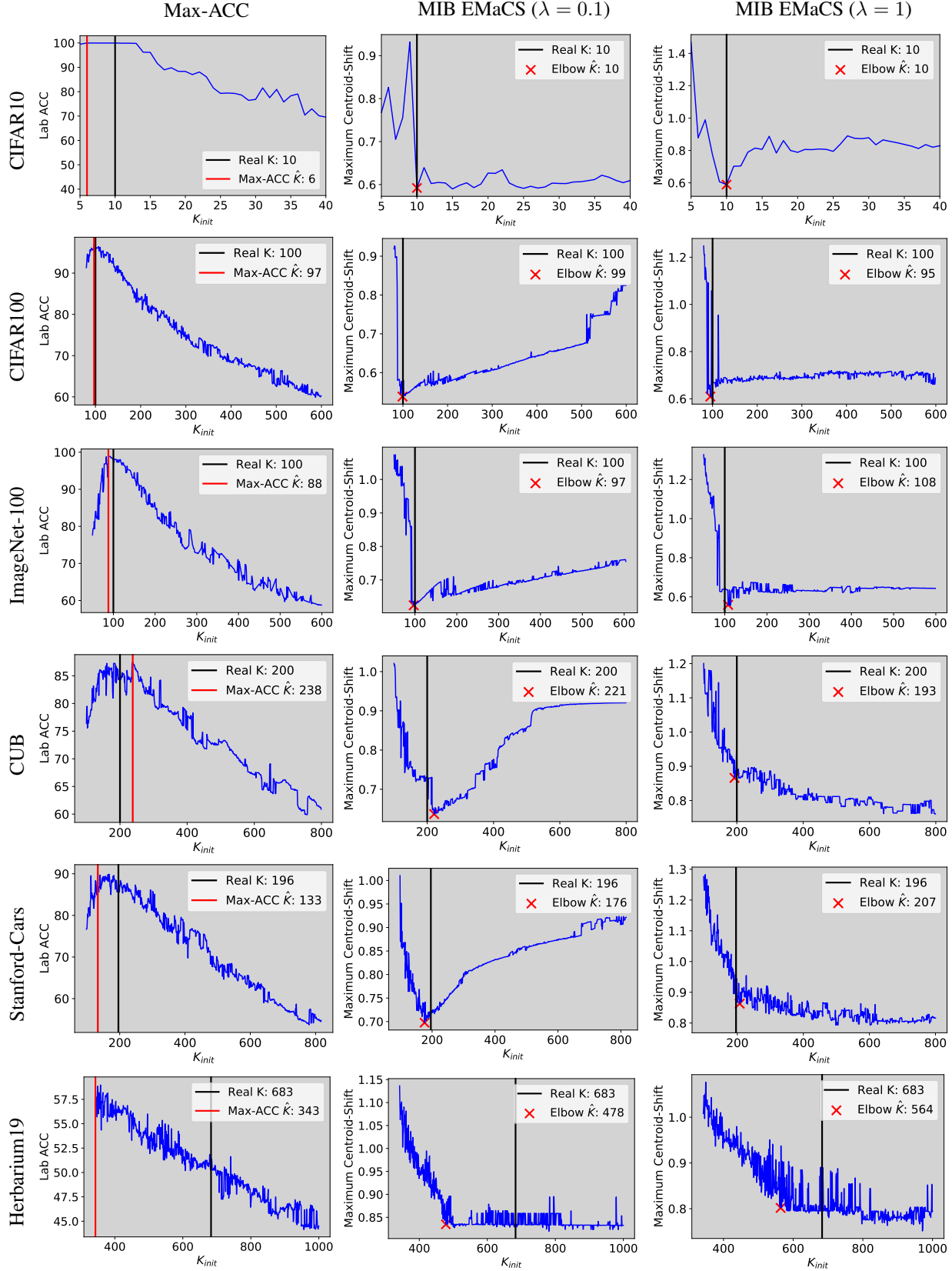


Figure 4. Comparison of Max-ACC [39] and proposed EMaCS strategies. We can observe that when using EMaCS with $\lambda = 0.1$ (2nd column), the Elbow point is more likely to also correspond to the minimum of the estimated curve, in particular on CIFAR100 (2nd row), ImageNet-100 (3rd row), CUB (4th row) and Stanford-Cars (5th row) datasets. *The reader can zoom on these figures on the pdf version.*